



**HAL**  
open science

# PDG-Arena: An ecophysiological model for characterizing tree-tree interactions in heterogeneous stands

Camille Rouet, Hendrik Davi, Arsène Druel, Bruno Fady, Xavier Morin

## ► To cite this version:

Camille Rouet, Hendrik Davi, Arsène Druel, Bruno Fady, Xavier Morin. PDG-Arena: An ecophysiological model for characterizing tree-tree interactions in heterogeneous stands. 2024. hal-04618761v1

**HAL Id: hal-04618761**

**<https://hal.inrae.fr/hal-04618761v1>**

Preprint submitted on 20 Jun 2024 (v1), last revised 11 Sep 2024 (v2)

**HAL** is a multi-disciplinary open access archive for the deposit and dissemination of scientific research documents, whether they are published or not. The documents may come from teaching and research institutions in France or abroad, or from public or private research centers.

L'archive ouverte pluridisciplinaire **HAL**, est destinée au dépôt et à la diffusion de documents scientifiques de niveau recherche, publiés ou non, émanant des établissements d'enseignement et de recherche français ou étrangers, des laboratoires publics ou privés.



Distributed under a Creative Commons Attribution - NonCommercial 4.0 International License

# PDG-Arena: An ecophysiological model for characterizing tree-tree interactions in heterogeneous stands

 Camille Rouet<sup>a,b,\*</sup>,  Hendrik Davi<sup>a</sup>,  Arsène Druel<sup>a</sup>,  Bruno Fady<sup>a</sup>,  
 Xavier Morin<sup>c</sup>

<sup>a</sup>INRAE URFM, Domaine Saint Paul – Site Agroparc, Avignon CEDEX 9, 84914, FRANCE

<sup>b</sup>ADEME, 20 avenue du Grésillé, Angers CEDEX 1, 49004, FRANCE

<sup>c</sup>CEFE, CNRS, Univ. Montpellier, EPHE, IRD, Montpellier, France, 1919 route de Mende, Montpellier CEDEX 5, 34293, FRANCE

---

## Abstract


In the context of ongoing climate and biodiversity crises, mixed forest stands are increasingly considered as a sustainable management alternative to monocultures. We developed a new individual-based and process-based forest growth model, PDG-Arena, to simulate mixed forest functioning and test ecophysiological interactions among trees in mixed stands. The model builds upon of a validated ecophysiological stand-scale model and integrates tree competition for light and water. We evaluated the simulation performance of PDG-Arena using annual growth data from 39 common beech and silver fir monospecific and mixed plots in the French Alps. PDG-Arena showed similar performance as the validated stand-scale model when simulating even-age and monospecific forests, and significantly better performance when using structure-diverse and species-diverse inventories. It also showed a significant positive effect of species mixing on gross primary production, canopy absorbance and transpiration. Our results thus show that tree-level process-based models such as PDG-Arena, formally simulating interspecific interactions, are needed to better understand and simulate the functioning of mixed stands.

**Keywords:** ecophysiology, process-based modeling, mixed forest, competition, biodiversity, overyielding, drought, ray-tracing, French Alps

---

---

\*Corresponding author

Email address: [contact.camille.rouet@pm.me](mailto:contact.camille.rouet@pm.me) ( Camille Rouet)

## Contents

<b>1</b>	<b>Introduction</b>	<b>3</b>
<b>2</b>	<b>Materials &amp; Methods</b>	<b>7</b>
2.1	Model description . . . . .	7
2.1.1	From CASTANEA to PDG-Arena . . . . .	7
2.1.2	Competition for water . . . . .	11
2.1.3	Competition for light . . . . .	12
2.2	Data set . . . . .	16
2.3	Simulation plan . . . . .	17
2.4	Model evaluation . . . . .	18
<b>3</b>	<b>Results</b>	<b>19</b>
3.1	Comparison of the simulation modalities . . . . .	19
3.2	Modeling performance . . . . .	19
3.3	Net biodiversity effect . . . . .	22
<b>4</b>	<b>Discussion</b>	<b>23</b>
<b>5</b>	<b>Declarations</b>	<b>28</b>
5.1	Declaration of competing interest . . . . .	28
5.2	Funding source . . . . .	28
5.3	Credits . . . . .	28
5.4	Author contributions . . . . .	28
<b>Appendix A</b>	<b>Supplementary description of PDG-Arena</b>	<b>29</b>
Appendix A.1	Computing of Leaf Mass per Area . . . . .	29
Appendix A.2	Estimation of the attenuation coefficient with reverse-engineering . . . . .	30
Appendix A.3	Distribution of radiations into canopy layers and into sun and shade leaves . . . . .	33
Appendix A.4	Reduction of absorbed radiations in SamsaraLight . . . . .	36
<b>Appendix B</b>	<b>Supplementary figures</b>	<b>37</b>

## 1. Introduction

1        Understanding how forest ecosystems function is a crucial step for develop-  
2        ing forest management strategies adapted to the challenges of global change,  
3        particularly climate change ([Bonan, 2008](#); [Lindner et al., 2010](#); [Trumbore et al.,](#)  
4        [2015](#)). In this context, mixed forests, in comparison with monospecific stands,  
5        have received increasing attention due to their documented ability to maintain  
6        key ecosystem services while enhancing stand resilience ([van der Plas et al., 2016](#);  
7        [Seynave et al., 2018](#); [Messier et al., 2022](#); [del Río et al., 2022](#)).

8        However, the physiological functioning of mixed stands is still poorly under-  
9        stood ([Forrester, 2014](#); [Forrester and Bauhus, 2016](#)). In particular, if species mix-  
10        ing seems on average to increase stand productivity in comparison to monospe-  
11        cific stands (a phenomenon known asoveryielding) ([Liang et al., 2016](#); [Zhang](#)  
12        [et al., 2012](#); [Vilà et al., 2007](#); [Forrester and Bauhus, 2016](#); [Piotto, 2008](#)), this  
13        trend depends on stand structure and species composition ([Zhang et al., 2012](#);  
14        [Ratcliffe et al., 2015](#)), as well as abiotic conditions ([Ratcliffe et al., 2016](#); [Toïgo](#)  
15        [et al., 2015](#)). Regarding the effect of diversity on the resistance of stands to  
16        drought episodes, the literature shows heterogeneous results ([Grossiord, 2018](#)).  
17        Indeed, the direction of the effect seems to depend on the species composition  
18        - and particularly on the species respective strategies in reaction to water stress  
19        ([Pretzsch et al., 2013](#); [Mas et al., 2024](#); [Jourdan et al., 2020](#)) - as well as on  
20        environmental conditions ([Grossiord et al., 2014](#); [Forrester et al., 2016](#); [Pardos](#)  
21        [et al., 2021](#)).

22        Stand structure, particularly tree density and size variability, can act as a  
23        confounding factor in the diversity-functioning relationships ([Metz et al., 2016](#);  
24        [Dănescu et al., 2016](#); [Cordonnier et al., 2019](#); [Zeller and Pretzsch, 2019](#)). To

25 better understand the processes underlying these relationships, it is therefore  
26 important to separate the effects of mixing related to differences in stand struc-  
27 ture (age, size, diameter) from those related to differences in the physiological  
28 functioning of species (crown architecture, water strategy, nutrient use, etc.)  
29 ([Forrester and Bausch, 2016](#)).

30 Furthermore, the types of interactions observed in a mixture may be of a  
31 different nature ([Forrester et al., 2016](#)), which could give rise to contradictory  
32 effects. For example, an increase in the amount of light captured in mixtures  
33 - e.g., through crown complementarity and plasticity, see [Jucker et al. \(2015\)](#) -  
34 could lead to an increase in gross primary production, but also in transpiration,  
35 with a potentially negative effect on drought resistance ([Jucker et al., 2014](#)).  
36 [Forrester \(2014\)](#) proposed a conceptual model to account for the mechanisms of  
37 interaction between diversity, functioning and environment. In this framework,  
38 interspecific interactions resulting in reduced competition for a given type of  
39 resource generates beneficial effects for individuals when this resource becomes  
40 scarce.

41 Assessing and predicting the functioning of mixed stands therefore requires  
42 detailed knowledge of interspecific interactions. This knowledge must be based  
43 on interactions between individuals and on the ecophysiological processes un-  
44 derlying these interactions, i.e. the processes determining competition for light,  
45 water and nutrients ([Pretzsch et al., 2017](#); [Grossiord, 2018](#)). Furthermore, a  
46 detailed understanding of the physiological mechanisms governing the diversity-  
47 functioning relationships in forests is all the more necessary as abiotic and biotic  
48 conditions, in which tree and species interactions take place, are and will be  
49 transformed by global change ([Ammer, 2019](#)).

50 Although experimental and observational systems are necessary for studying  
51 the biodiversity-functioning relationship in forests, they are limited by their sample  
52 size, measurement completeness and number of confounding factor that can  
53 be controlled ([Bauhus et al., 2017](#)). Modeling can virtually overcome these  
54 limitations, subject to the assumptions contained in the model, which depend  
55 to a large extent on our ecological knowledge as well as on the availability of  
56 climatic, pedological, silvicultural and physiological data. This approach has been  
57 used to put forward hypotheses to explainoveryielding in mixing. For example  
58 [Morin et al. \(2011\)](#) showed with simulations thatoveryielding could be explained  
59 by the diversity of species traits related to shade-tolerance, maximum height  
60 and growth rate (although other explanations were not ruled out). Simulations  
61 also make it possible to virtually assess the stability of the productivity of forest  
62 mixtures while testing numerous community composition ([Morin et al., 2014](#)),  
63 even under unprecedented climatic conditions ([Jourdan et al., 2021](#)).

64 The literature ([Korzukhin et al., 1996](#); [Cuddington et al., 2013](#); [Morin et al.,](#)  
65 [2021](#)) depicts a spectrum going from empirical models, based on relationships  
66 calibrated from observations between final variables such as productivity and  
67 explanatory variables (rainfall, sunshine, etc.), to process-based models whose  
68 final variables are computed using explicit elementary processes (photosynthesis,  
69 transpiration, phenology, etc.). For some authors ([Fontes et al., 2010](#); [Cud-](#)  
70 [dington et al., 2013](#); [Korzukhin et al., 1996](#)), process-based models, because of  
71 their supposed greater versatility, seem more relevant for simulating ecosystem  
72 functioning undergoing climate change. As a result, they now play an important  
73 role in research into the functioning and predicting of forest ecosystem dynam-  
74 ics ([Gonçalves et al., 2021](#)). When it comes to simulate mixed stands, models

75 that simulate elementary processes theoretically have a better ability to repro-  
76 duce the mechanisms that lead to interspecific interactions, bringing us closer to  
77 understanding them ([Forrester and Bauhus, 2016](#)).

78 Among process-based models, a distinction is made between individual-based  
79 models, e.g. [Jonard et al. \(2020\)](#), and stand-scale models, e.g. [Dufrêne et al.](#)  
80 [\(2005\)](#). Several biodiversity-functioning studies in forests have highlighted the  
81 importance of tree-tree interactions in defining the nature of interspecific inter-  
82 actions at the stand level ([Trogisch et al., 2021](#); [Jourdan et al., 2020](#); [Guillemot](#)  
83 [et al., 2020](#); [Jucker et al., 2015](#)). Thus, the individual scale appears relevant for  
84 representing the key mechanisms that govern the functioning of mixed forests  
85 ([Porté and Bartelink, 2002](#)). Finally, process-based and individual-based mod-  
86 els have the ability to distinguish the effects of competition between individuals  
87 with different functions (mixing effect) and the effects of competition between  
88 individuals of different sizes (structure effect). So far, few models are able to  
89 simulate mixed stands by taking advantage of both physiological mechanisms  
90 and the individual scale ([Reyer, 2015](#); [Pretzsch et al., 2015](#)).

91 Here we present PDG-Arena, a new individual-based, process-based, forest  
92 growth model. Our model was developed to observe the stand scale properties  
93 that emerge when trees of different species and size compete in a given environ-  
94 ment. It was therefore built: (i) from elementary physiological processes using  
95 the stand-scale model CASTANEA ([Dufrêne et al., 2005](#)) and (ii) by integrating  
96 elementary interaction mechanisms among trees, notably competition for light  
97 and water. PDG-Arena is designed as an extension of Physio-Demo-Genetics  
98 (denoted PDG), a model developed on the Capsis modeling platform ([Oddou-](#)  
99 [Muratorio and Davi, 2014](#); [Dufour-Kowalski et al., 2012](#)).

100 The performance of PDG-Arena was evaluated using annual growth data from  
101 a monitoring network of monospecific and multispecific stands of common beech  
102 (*Fagus sylvatica* L.) and silver fir (*Abies alba* Mill.). Firstly, we tested whether  
103 PDG-Arena, despite increased complexity, accurately reproduces the performance  
104 of CASTANEA when both models are run under comparable conditions. Sec-  
105 ondly, we evaluated PDG-Arena's performance in different conditions in terms  
106 of stand structure and species diversity. Lastly, using PDG-Arena, we evaluated  
107 the net biodiversity effect (i.e. the effect of species mixing) on carbon, light and  
108 water processes.

## 109 2. Materials & Methods

### 110 2.1. Model description

#### 111 2.1.1. From CASTANEA to PDG-Arena

112 PDG-Arena was developed as an extension of PDG ([Oddou-Muratorio and](#)  
113 [Davi, 2014](#)) with the aim to simulate the functioning of a diverse, multispecific  
114 stand. PDG is an individual-based and spatially explicit model that combines: (1)  
115 the process-based model CASTANEA to simulate tree ecophysiological function-  
116 ing, (2) demographic processes allowing to model tree survival and reproduction  
117 and (3) a quantitative genetics simulation module accounting for the heritability  
118 and intraspecific diversity of key life history trait of the CASTANEA model. While  
119 PDG is built with the idea of simulating the evolutionary dynamic of functional  
120 traits, PDG-Arena is designed to simulate ecological interactions between trees.

121 CASTANEA is an ecophysiological forest growth model that simulates the  
122 dynamics of homogeneous stands (Figure 1a). Among others, it has been pa-  
123 rameterized and validated on common beech (*Fagus sylvatica* L., [Dufrêne et al.](#),



124 2005) and silver fir (*Abies alba* Mill., Davi and Cailleret, 2017). CASTANEA is  
125 composed of five equal-sized leaf layers that perform photosynthesis based on  
126 stomatal conductance and on the level of radiation received by each layer, which  
127 is determined using a horizontally homogeneous, multi-layer, radiation model.  
128 The resulting gross primary production, minus autotrophic respiration, is then  
129 allocated into the leaf, fine root, coarse root, branch, trunk and reserves com-  
130 partments (Davi et al., 2009). The amount of leaf transpiration is determined by  
131 net radiation, stomatal conductance as well as ambient temperature and vapor  
132 pressure deficit. The stomatal conductance, limiting photosynthesis and tran-  
133 spiration, is controlled by soil water stress. Lastly, leaf phenology is controlled  
134 by day length and mean temperature. The temporal scale of the processes in  
135 CASTANEA are the same in PDG-Arena, as shown in Table 1.

Table 1: Temporal and spatial scales of physical and physiological processes in PDG-Arena.

	Tree level	Stand level
Hourly level	Photosynthesis	Ray casting
	Respiration	Soil evaporation
	Crown transpiration	
	Crown evaporation	
Daily level	Water interception	Water balance
	Leaf phenology	
	Carbon allocation	
Yearly level	Tree growth	

136 The existing model PDG considers isolated abstract trees, simulating the dy-  
137 namics of each of them using stand-scale CASTANEA processes. All quantitative  
138 physiological variables in CASTANEA and in PDG are related to the stand soil  
139 surface: eg, the gross primary production is expressed in  $\text{gC}/\text{m}^2$ . The first im-

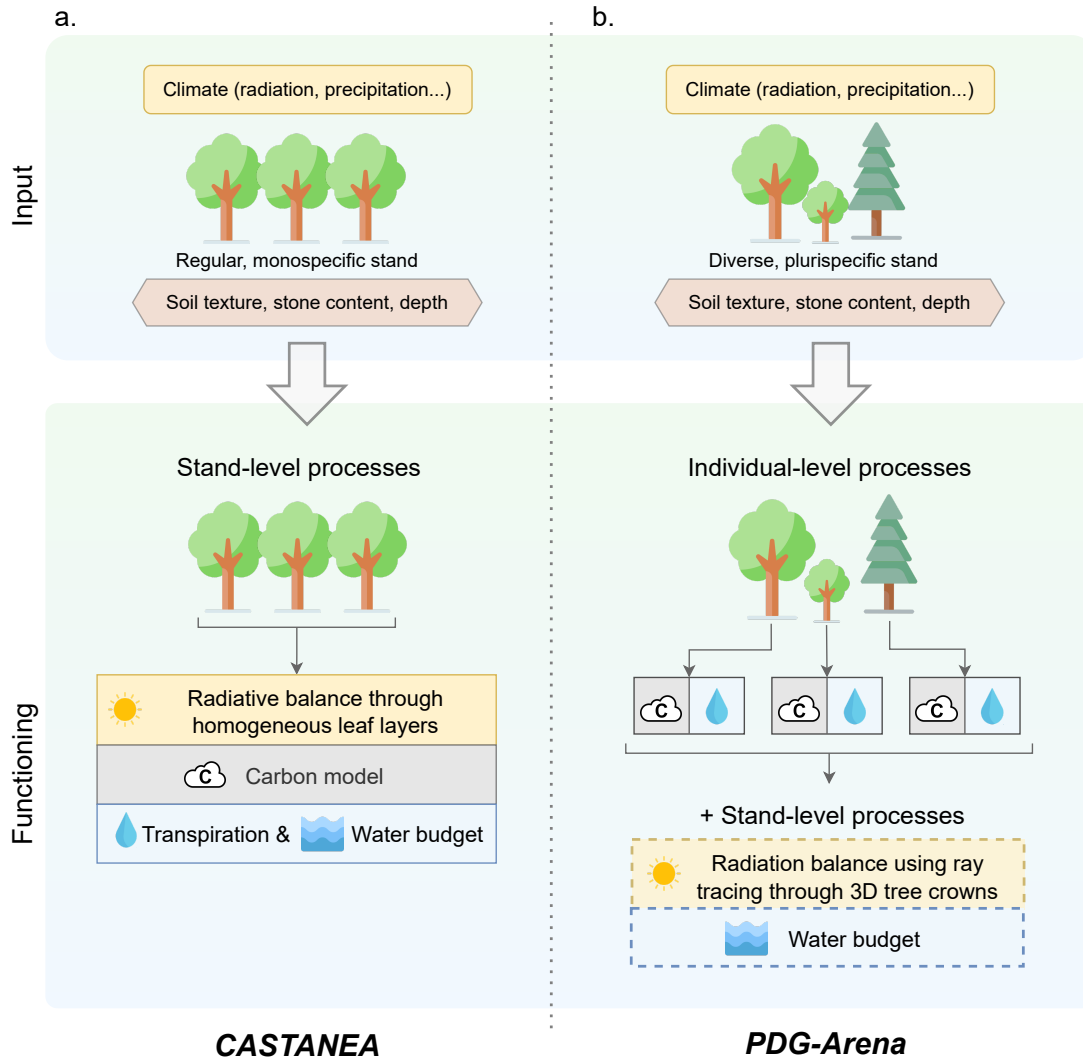


Figure 1: Conceptual diagram of the (a) CASTANEA and (b) PDG-Arena forest growth models input and functioning. CASTANEA simulates the growth of a regular monospecific stand whereas PDG-Arena simulates the dynamics of a diverse multispecific stand. In CASTANEA, all processes, including radiation balance with the SAIL model, carbon fluxes, trees transpiration and soil water budget are held at the stand level, on horizontally homogeneous leaf layers. PDG-Arena takes advantage of CASTANEA carbon and transpiration processes but hold them at the tree level, while a water budget is held at the stand level. The radiative balance is handled by the SamsaraLight library which casts light rays through a 3D representation of a trees crowns. Processes involving competition between trees in PDG-Arena are shown in dashed boxes.

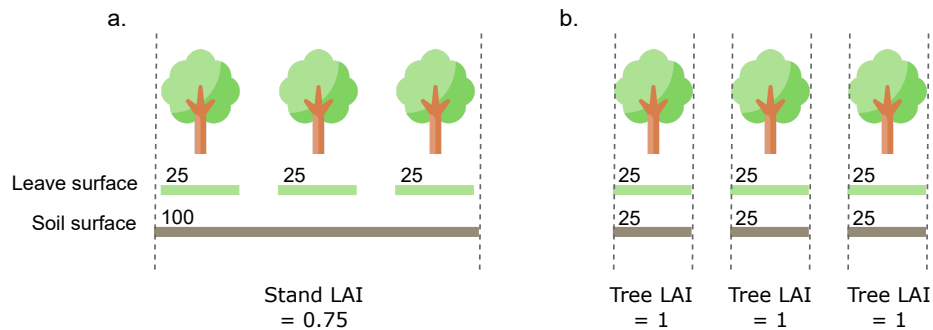


Figure 2: Difference in the representation of Leaf Area Index (LAI) between (a.) the stand-scale model CASTANEA and (b.) the individual-based model PDG-Arena. Values of leaf surface, soil surface and LAI are arbitrary.

140 improvement of PDG-Arena over PDG is that the physiological processes simulate  
141 tree functioning instead of stand functioning (Figure 1b). To do so, physiological  
142 processes are related to individual trees crown projection surface rather than to  
143 the stand soil area. This paradigm shift implied changing the definition of some  
144 variables. As depicted in Figure 2, the Leaf Area Index (LAI) is now defined for  
145 each tree as the amount of leaf surface of a tree per  $m^2$  of soil under its crown.  
146 While the stand LAI in CASTANEA depends on the amount of gap fraction,  
147 individual tree LAI in PDG-Arena does not: a tree's LAI only accounts for its leaf  
148 surface and its crown projection surface. The same reasoning applies to other  
149 physiological variables, such as carbon uptake, water transpiration, absorbed ra-  
150 diation, etc. Also, the Leaf Mass Area (LMA), as it depends on the amount of  
151 light intercepted by neighboring trees (Davi et al., 2008a), is computed at the  
152 individual level in PDG-Arena according to the vertical profile of the leaf area of  
153 neighboring trees (see Appendix A.1).

154 The second improvement of PDG-Arena over PDG is that it integrates mech-  
155 anisms of competition for light and water between neighboring trees (see Figure

156 1b) by: (i) making trees share the same stand soil water pool and (ii) simulating  
157 the radiative balance using a ray tracing model.

### 158 *2.1.2. Competition for water*

159 Competition for water is a crucial element in the water dynamics of mixed  
160 stands. We modeled competition for water symmetrically between individuals,  
161 i.e., trees in the same plot all draw from the same water reservoir without spa-  
162 tial differentiation, either horizontal (distance between individuals) or vertical  
163 (depth). The assumption for no horizontal differentiation is justified here by the  
164 small area of the modeled plot.

165 Every day of simulation, the stand-level volume of precipitation is divided  
166 into a portion that does not interact with the canopy – i.e., that falls directly  
167 to the ground – and another portion that reaches the canopy. The portion that  
168 interacts with the canopy is given by the proportion of soil that is directly under  
169 any tree crown. Then, this portion of precipitation is distributed among trees  
170 according to their respective leaf surface. For each tree, a calculation of drip,  
171 runoff, and precipitation passing through the crown is performed. Transpiration  
172 and crown evaporation of trees are calculated individually at the hourly time step  
173 using the Penman-Monteith equation (Monteith, 1965), taking into account the  
174 energy absorbed by individual crowns (section 2.1.3). Stand soil evaporation is  
175 computed at the hourly level and homogeneously along the plot.

176 Considering drip, runoff and water passing through the crowns on the one  
177 hand, and tree transpiration, canopy and soil evaporation and drainage on the  
178 other, a water balance is computed at the stand level each day (Table 1 and  
179 Figure 1b). Therefore, soil water status (soil moisture, litter moisture and soil  
180 potential) is the same for every tree within a plot on any given day.

181 *2.1.3. Competition for light*

182 Competition for light in PDG-Arena is performed using SamsaraLight, a ray  
183 tracing library derived from [Courbaud et al. \(2003\)](#) and maintained on the Cap-  
184 sis modeling platform. The integration of SamsaraLight with the physiological  
185 model CASTANEA (which is partly inspired from the approach in the HETERO-  
186 FOR model, [Jonard et al., 2020](#)) is described here. PDG-Arena operates two  
187 executions of SamsaraLight each year: in the PAR (photosynthetically active  
188 radiations) domain and in the NIR (near infrared radiations) domain. For one  
189 execution, SamsaraLight generates every year a set of diffuse and direct beams,  
190 and computes their interception by tree crowns and soil cells. The simulated  
191 energy absorbed by crowns is then temporally distributed at the hourly scale.  
192 The energy absorbed by a crown is distributed among its five leaf layers, which  
193 are part of a CASTANEA model for each tree.

194 *Definition of crowns.*

195 Each tree is represented by a trunk and a crown occupying a volume in space.  
196 Trunks are ignored in the radiation balance, while the characteristics of crowns  
197 are defined by the following parameters:

- 198 ● the height of the tree  $h$ ;
- 199 ● its crown base height,  $hcb$ ;
- 200 ● its crown radius *crownRadius*;
- 201 ● its shape, which is considered as conical in the case of Fir and ellipsoidal  
202 in the case of Beech (shapes are vertically bounded by  $h$  and  $hcb$  and  
203 horizontally bounded by *crownRadius*);

- 204 • its leaf area density at period of full vegetation, denoted  $LAD$ , in  $\text{m}^2$  of  
205 leaf per  $\text{m}^3$  of crown volume;
- 206 • its attenuation coefficient  $k$ ;
- 207 • its clumping index  $\Omega$  defining the aggregation of the leaves inside the crown.

208 Trees  $h$  and  $hcb$  are inputs of the model (section 2.2). Trees crown radius  
209 are determined using an allometric relationship based on species and diameter at  
210 breast height (DBH):

$$crownRadius = \beta_{crown} + \alpha_{crown} \times DBH \quad (1)$$

211  $\alpha_{crown}$  and  $\beta_{crown}$  are species dependent parameters estimated on site at  
212 Mont Ventoux (unpublished data from one of the authors, H. Davi).  $\Omega$  is species  
213 dependent and was measured on Mont Ventoux sites by [Davi et al. \(2008b\)](#). The  
214  $LAD$  of a tree is the ratio of its maximum leaf area to its crown volume. The  
215 leaf area of a given tree  $i$  (denoted  $LA_i$ ) is determined as a portion of its stand  
216 leaf area ( $LA_{stand}$ ). All stand leaf surfaces were measured using Terrestrial Laser  
217 Scanning in the summers of 2022 and 2023 (unpublished data from one of the  
218 authors, C. Rouet). For every tree, its portion of leaf area is proportional to  
219 its theoretical leaf area  $LA_{th}$ , which is given by an allometric equation based on  
220 species and DBH from [Forrester et al. \(2017b\)](#).

221 The attenuation coefficient  $k$  depends on species, radiation domain, type of  
222 radiation (direct, diffuse) and beam height angle. Its value is determined using  
223 reverse-engineering of SAIL, the radiation sub-model in CASTANEA, as described  
224 in [Appendix A.2](#).

225 *Ray casting.*

226 SamsaraLight generates two set of beams. Firstly, diffuse rays are distributed  
227 in all the directions at regular interval of 5°. Secondly, direct rays are generated  
228 to follow the hourly trajectory of the sun for one virtual day per month. Each  
229 set of beams contains the energy of the entire year for both diffuse and direct  
230 radiation. The stand plot is subdivided into square cells of 1.5m width. All beams  
231 are replicated for each ground cell, aiming at the center of the cell.

232 Once all the rays have been created, SamsaraLight performs the ray casting  
233 as described in [Courbaud et al. \(2003\)](#). For each ray, its energy is attenuated  
234 when it crosses an obstacle (in our case, a crown). The proportion of energy  
235 transmitted follows the formulation of the Beer-Lambert law:

$$I_T = I_0 e^{-k \times \Omega \times LAD \times l_p} \quad (2)$$

236 where  $l_p$  is the path length of the ray in the crown and  $I_0$  is the energy of the  
237 beam before it intercepts the crown. Then, the energy absorbed by a crown  $I_A$   
238 is the complement of the transmitted energy:

$$I_A = I_0 - I_T \quad (3)$$

239 Note that SamsaraLight does not take directly into account the reflection  
240 of light - which causes a loss of energy in the sky and a reabsorption of the  
241 energy reflected on the ground. These phenomena are taken into account when  
242 calculating the attenuation coefficient.

243 After interception by a crown, the ray continues its course until it reaches  
244 either a new crown or a ground cell to which the remaining energy of the ray is

245 transmitted. At the end of the ray casting, we know for each crown and each  
246 soil cell the amount of direct and diffuse energy received in a year.

247 *Computation of hourly absorbed energy.*

248 The hourly absorbed radiation of any element is then computed using the ray  
249 casting on the one hand and the hourly incident radiation on the other hand.

250 For each absorbing element  $i$  (a soil cell or a tree crown) and for each type of  
251 radiation (direct/diffused, PAR/NIR), the energy it absorbs at the hourly scale is  
252 given by the hourly incident radiation  $gr(h)$  and the fraction of energy absorbed  
253 annually by this element,  $I_{Ay}(i)$ , divided by the total energy absorbed by all  
254 elements  $j$  over the year:

$$I_A(h, i) = gr(h) \times \frac{I_{Ay}(i)}{\sum_j I_{Ay}(j)} \quad (4)$$

255 The value of  $I_A(h, i)$  has then to be amended because the ray casting used  
256 values of LAD that assume trees were at their period of full vegetation. A surplus  
257 of energy is then removed afterward from each tree according to their daily level  
258 of leaf development. This surplus is redistributed into other trees and soil cells,  
259 as described in [Appendix A.4](#).

260 *Distribution into layers.*

261 Within a real-life tree, some leaves can receive a large amount of light -  
262 which leads to a saturation of the photosynthesis capacities - while other leaves  
263 are in the shade. The saturation phenomenon (and more generally the concavity  
264 of the absorbed light-photosynthesis relation) forbids calculating photosynthesis  
265 by considering an average level of light absorption for the whole canopy: this  
266 would bias upwards the evaluation of photosynthesis ([Leuning et al., 1995](#)). In



267 CASTANEA, the energy absorbed by the canopy is therefore distributed into  
 268 five layers of leaves, in which the absorbed energy is assumed to be relatively  
 269 homogeneous. The layers are themselves divided between leaves in direct light  
 270 (called sun leaves) and leaves in the shade. The distribution of energy into layers  
 271 is described in [Appendix A.3](#).

## 272 2.2. Data set

273 The simulations were evaluated at plot scale using dendrochronological data  
 274 obtained on beech, fir and beech-fir stands from the French pre-Alps (GMAP  
 275 forest plot design, [Jourdan et al., 2019, 2020](#)). The data set includes 39 plots of  
 276 10 m radius distributed on three sites (Bauges, Ventoux, Vercors) as described  
 277 in [Table 2](#), and represents the annual growth dynamics of 1177 stems over the  
 278 18-year period 1996-2013. Wood volume increments are obtained by multiplying  
 279 the individual basal area increments by each tree height. Finally, we used the  
 280 wood volume increments per stand to evaluate the simulations.

Table 2: Characteristics of the stands used to evaluate the model. Mean value and standard deviation for each site (Bauges, Ventoux, Vercors, all) and composition (Mixed, Beech, Fir, all) are shown for variables: number of stands, altitude (in m), mean diameter at breast height per stand (in cm), density (in stem/ha), basal area (in m<sup>2</sup>/ha), proportion of beech basal area (in %), mean age per stand, Leaf Area Index (in m<sup>2</sup>/m<sup>2</sup>).

Site / Composition	N	altitude	mean DBH	density	basal area	% beech	mean age	LAI
Bauges	10	1100 ± 101	28.7 ± 6.7	1030 ± 685	72 ± 14	0.53 ± 0.43	89 ± 16	3.0 ± 0.4
Vercors	14	1250 ± 101	32.3 ± 8.6	657 ± 275	56 ± 14	0.53 ± 0.38	118 ± 40	3.0 ± 0.8
Ventoux	15	1250 ± 126	22.1 ± 6.3	1450 ± 623	57 ± 13	0.50 ± 0.40	105 ± 47	2.9 ± 0.5
Mixed	13	1200 ± 131	26.2 ± 7.3	1080 ± 465	64 ± 13	0.46 ± 0.10	101 ± 29	2.6 ± 0.5
Beech	14	1230 ± 118	26.7 ± 10.3	1200 ± 794	56 ± 14	0.97 ± 0.05	119 ± 35	3.3 ± 0.6
Fir	12	1190 ± 139	29.8 ± 7.4	867 ± 578	62 ± 18	0.05 ± 0.07	94 ± 50	2.9 ± 0.6
all	39	1210 ± 126	27.5 ± 8.4	850 ± 632	60 ± 15	0.51 ± 0.39	105 ± 39	2.9 ± 0.6

281 Field inventories include the position, height, crown base height, age, diam-  
282 eter and species of every tree with DBH greater than 7.5 cm in each of the 39  
283 stands. Hourly climate data (temperature, global radiation, wind speed, pre-  
284 cipitation and relative humidity) were obtained from the 8 km scale SAFRAN  
285 reanalysis dataset (Vidal et al., 2010) for the three sites and temperatures were  
286 adapted to each stand altitude using an adjustment of 0.6 °C/100m (Rolland,  
287 2003). Soil texture, depth and stone content were obtained for every stand  
288 (unpublished data from one of the authors, X. Morin).

### 289 *2.3. Simulation plan*

290 Using field inventories, we generated three sets of virtual inventories for PDG-  
291 Arena, following three levels of abstraction, denoted RN, RS and O. The first  
292 set represents regularized inventories with no species interactions (RN): for each  
293 species of each stand, we generated a new inventory with equally spaced trees of  
294 the same species, age, diameter and height. The simulation results using regular  
295 monospecific inventories generated from the same stand were then assembled  
296 relatively to the proportion of each species basal area. RN inventories can then be  
297 used to simulate the growth of multispecific stands, ignoring species interactions.  
298 The second set represents regularized inventories with species interactions (RS):  
299 trees of the same species share the same age, diameter and height. Plus, trees  
300 are regularly spaced in a random order, independently of the species. Lastly,  
301 original inventories (O) include the information of the real life dataset, that is:  
302 species, position, diameter and height of every individual trees. For each type  
303 of inventories representing the same stand (regularized or not, with or without  
304 species interactions), the mean quadratic diameter, volume per tree and tree age  
305 per species and the basal area were conserved.

306 CASTANEA was used as a reference model to evaluate the performance  
307 enhancement brought by PDG-Arena. We used regularized inventories with no  
308 species interactions (RN) for CASTANEA's stand-scale simulations. It is to be  
309 noted that, contrary to PDG-Arena, CASTANEA does not account for the stand  
310 slope. Therefore, when comparing CASTANEA and PDG-Arena results (section  
311 [3.1](#)), the slope was put to zero in PDG-Arena inventories. In the other situations  
312 (sections [3.2](#) and [3.3](#)), the slopes of the inventories simulated using PDG-Arena  
313 were those of the field data.

314 To sum up, we simulated the growth of 39 stands over the 18-year period  
315 1996-2013, considering four modeling situations: RN, RS and O inventories with  
316 PDG-Arena on the one hand, and RN inventories with CASTANEA on the other  
317 hand. Tree reproduction and intraspecific diversity, which are characteristics of  
318 PDG and therefore PDG-Arena, were switched off for these simulations. Inven-  
319 tories, simulation results and the analysis script were deposited on the Zenodo  
320 repository platform ([Rouet, 2024](#)).

#### 321 *2.4. Model evaluation*

322 To evaluate the similarity between each modeling situation, we used the  
323 gross primary production (GPP) as CASTANEA and PDG-Arena are carbon-  
324 based models. We computed the coefficient of correlation ( $r$ , from -1 to 1) for  
325 the simulated GPP per stand between the four situations of simulation.

326 To evaluate the performance of the models against field measurements, we  
327 used the simulated wood volume increment per stand. We computed the Mean  
328 Absolute Percent Error (MAPE) and the coefficient of determination ( $r^2$ , from  
329 0 to 1) between simulations and measurements. A low MAPE indicates that  
330 simulated wood production is on average close to measured production. A  $r^2$

331 close to 1 shows a good capacity of the model to predict the stand production  
332 variability.

333 Lastly, we evaluated the net biodiversity effect (NBE) to inform us about the  
334 presence of physiological processes that are caused by species mixing. It is defined  
335 as the difference for a variable between its observed value in mixed stands and its  
336 predicted value based on the hypothesis that there is no complementarity effect  
337 between species (Loreau, 2010). Here, we compared the value of a simulated  
338 variable with PDG-Arena using RS and RN inventories. The NBE was evaluated  
339 on GPP, canopy absorbance, transpiration rate and water shortage level (defined  
340 as the maximum difference reached during simulation between the current and  
341 full useful reserve, in mm). The NBE was tested against the null hypothesis  
342 using two-sided Wilcoxon signed rank test.

### 343 **3. Results**

#### 344 *3.1. Comparison of the simulation modalities*

345 Using regularized inventories with no species interactions (RN), CASTANEA  
346 and PDG-Arena showed similar predictions for the stand-level GPP, as represented  
347 in Figure 3. The coefficient of correlation between the two models was estimated  
348 at 99.6%. Moreover, as shown in Table 3, which compares the 4 modeling  
349 situations based on the coefficient of determination, PDG-Arena was closer to  
350 CASTANEA when using regularized stands and when species interactions were  
351 disabled.

#### 352 *3.2. Modeling performance*

353 Performances of CASTANEA's and PDG-Arena's simulations against mea-  
354 sured wood volume increment per stand are reported in Table 4. Firstly, PDG-

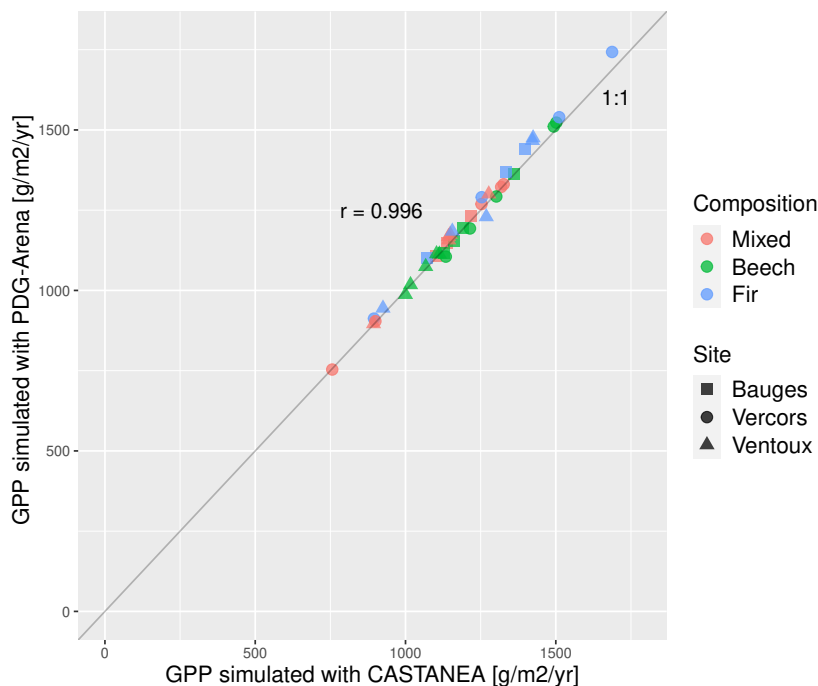


Figure 3: Gross primary production (GPP) per stand simulated by PDG-Arena and CASTANEA. Regularized inventories with no species interactions (RN) were used.  $r$  is the correlation coefficient.

Table 3: Matrix of similarity between simulated GPP from CASTANEA and PDG-Arena using different types of inventories: 'RN' (regularized with no species interactions), 'RS' (regularized with species interactions) and 'O' (original inventories). Similarity is expressed using the correlation coefficient (in %) of the simulated gross primary production for the 39 stands over the 1996-2013 period.

	CASTANEA (RN)	PDG-Arena (RN)	PDG-Arena (RS)	PDG-Arena (O)
CASTANEA (RN)	100.0	-	-	-
PDG-Arena (RN)	99.6	100.0	-	-
PDG-Arena (RS)	98.4	99.0	100.0	-
PDG-Arena (O)	96.5	97.4	98.4	100.0

Table 4: Evaluation of the performances of PDG-Arena and CASTANEA. Coefficient of determination ( $r^2$ , in %) and Mean Absolute Percent Error (MAPE, in %) were computed for the simulated versus measured yearly wood volume increment per stand over the period 1996-2013. Inventories are characterized as: 'RN' (regularized with no species interactions), 'RS' (regularized with species interactions) and 'O' (original inventories).

Set	Model	Inventories	$r^2$	MAPE
All stands	CASTANEA	RN	17.6	44.0
	PDG-Arena	RN	18.4	43.0
	PDG-Arena	RS	19.0	43.2
	PDG-Arena	O	20.9	40.5
Mixed	CASTANEA	RN	40.2	36.4
	PDG-Arena	RN	40.3	37.8
	PDG-Arena	RS	43.1	38.9
	PDG-Arena	O	50.1	34.1
Beech pure	CASTANEA	RN	22.0	53.1
	PDG-Arena	RN	21.6	51.6
	PDG-Arena	RS	21.6	51.9
	PDG-Arena	O	36.2	47.0
Fir pure	CASTANEA	RN	7.8	41.5
	PDG-Arena	RN	12.5	38.5
	PDG-Arena	RS	11.5	37.8
	PDG-Arena	O	12.9	40.0

355 Arena gave slightly better performances than CASTANEA on comparable inven-  
356 tories, i.e. RN inventories ( $r^2$  18.4 vs 17.6%, MAPE 43.0 vs 44.0%). Using the  
357 original stand dataset (O), PDG-Arena performed better than CASTANEA ( $r^2$   
358 20.9% vs 17.6%, MAPE 40.5% vs 44.0%), with particularly better predictions  
359 for mixed ( $r^2$  50.1 vs 40.2%, MAPE 34.1 vs 36.4%) and beech stands ( $r^2$  36.2  
360 vs 22.0%, MAPE 47.0 vs 53.1%). Both PDG-Arena using O inventories and  
361 CASTANEA using RN inventories had poor prediction capacity for the fir stands,  
362 although PDG-Arena performed better than CASTANEA ( $r^2$  at 12.9% vs 7.8%).  
363 The mean absolute error was larger for beech stands, moderate for fir stands and  
364 lower for mixed stands: respectively, 53.1%, 41.5% and 36.4% for CASTANEA  
365 and 47.0%, 40.0% and 34.1% for PDG-Arena using O inventories.

366 Activation of species interactions in PDG-Arena (RS vs RN inventories) en-  
367 hanced the  $r^2$  on mixed stands (43.1 vs 40.3%) but also slightly increased the  
368 mean absolute error (38.9 vs 37.8%). Using original instead of regularized in-  
369 ventories (O vs RS), PDG-Arena gave better performances on mixed ( $r^2$  50.1  
370 vs 43.1%, MAPE 34.1 vs 38.9%) and beech ( $r^2$  36.2 vs 21.6%, MAPE 47.0 vs  
371 51.9%) stands and similar performance on fir stands ( $r^2$  12.9 vs 11.5%, MAPE  
372 40 vs 37.8%).

### 373 3.3. Net biodiversity effect

374 The GPP and canopy absorbance simulated by PDG-Arena in mixed stands  
375 are represented in Figure 4 for RN, RS and O inventories. Additionally, Figure B.7  
376 shows the maximum water shortage and yearly transpiration rate. Comparison of  
377 simulations with RS and RN inventories showed a positive net biodiversity effect  
378 on GPP (1180 vs 1110 gC/m<sup>2</sup>/year; p-value < 0.001) and canopy absorbance  
379 (0.332 vs 0.302; p-value < 0.001), but also on canopy transpiration (171 vs 150

380 mm; p-value < 0.001) and maximum water shortage (74.8 vs 67.6 mm; p-value  
381 < 0.001). The mixing effect, i.e. the fact of simulating species in interaction  
382 instead of separately, thus increased the GPP and canopy absorbance of 6.1%  
383 and 10.1% respectively, and also increased the transpiration and water shortage  
384 of 14.0% and 10.7%, respectively.

385 The structure effect (evaluated by comparing O and RS inventories on all 39  
386 stands, not shown here) slightly decreased the GPP (1180 vs 1220 gC/m<sup>2</sup>/year;  
387 p-value < 10<sup>-4</sup>) and canopy absorbance (0.316 % vs 0.330%; p-value < 10<sup>-4</sup>).  
388 Transpiration also showed a slight decrease (167 vs 172 mm; p-value < 10<sup>-4</sup>)  
389 and maximum water shortage showed no significant variation (74.7 vs 75.5 mm;  
390 p-value > 0.05).

#### 391 4. Discussion

392 Given the paucity of forest growth models simulating ecophysiological pro-  
393 cesses at the individual scale, we developed the individual-based model PDG-  
394 Arena from the stand-scale model CASTANEA in order to simulate mixed forests.  
395 PDG-Arena was built with the idea of observing and understanding the proper-  
396 ties that emerge in multispecific stands. It uses on the one hand a physiological  
397 model parameterized for monospecific stands and on the other hand an individual  
398 scale structure that allows trees to interact - the interaction being more or less  
399 competitive depending on the functional traits of the individuals and species.

400 We showed that PDG-Arena was able to reproduce the behavior of CAS-  
401 TANEA when simulating regularized inventories with no species interactions.  
402 Thus, the increase in complexity of PDG-Arena, made necessary in order to  
403 simulate the functioning and interactions of distinct trees, was not at the cost



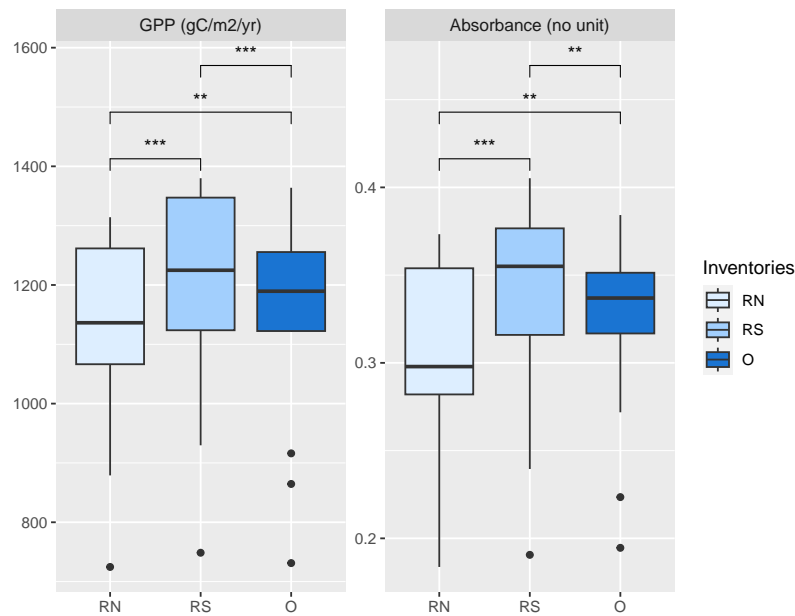


Figure 4: Gross primary production (GPP) and canopy absorbance simulated by PDG-Arena for 13 mixed stands. Three types of inventories were used: regularized inventories with no species interactions (RN), regularized inventories with species interactions (RS) and original inventories (O). Two-sided Wilcoxon signed rank test was used (\*\*: p-value < 0.01, \*\*\*: p-value < 0.001).

404 of decreased performance at the stand scale. PDG-Arena, in comparison to  
405 CASTANEA, is able to account for stands' irregular structure and diversity in  
406 species and showed better performance, particularly on beech ( $r^2$  +14.2 per-  
407 centage points) and mixed stands ( $r^2$  +9.9 percentage points). Moreover, as  
408 shown by the simulations using different types of inventories, the improvement  
409 in simulating stand growth is explained by both the integration of interspecific  
410 interactions and the use of the original stand structure.

411 The performance of both CASTANEA and PDG-Arena at predicting the vari-  
412 ability of fir stands productivity remained poor ( $r^2 < 13\%$ ). This can possibly be  
413 explained by the presence of three fir stands from the Bauges site that showed  
414 particularly large measured growth, a pattern that was not predicted by the mod-  
415 els (see Figures B.5 and B.6). The mismatch could result from the time elapsed  
416 between the year of measured growth (1996-2013) and the year of measurement  
417 of the Leaf Area Index (2022 for the Bauges site), that drives CASTANEA phys-  
418 iological processes. The value of LAI we measured reflects recent extreme hot  
419 and dry events ([Rakovec et al., 2022](#)) that the growth data necessarily did not  
420 capture.

421 Interestingly, a positive and significant net biodiversity effect was observed in  
422 PDG-Arena simulations on gross primary productivity by comparing simulations  
423 with interacting species to equivalent simulations with species in isolation. The  
424 simulated overyielding can be attributed to an improvement of canopy absorbance  
425 due to species mixing (Figure 4). Leaf area being equal between each simulation  
426 modality for the same stand, the increased light absorption is explained by a  
427 greater occupation of the aerial space in mixed stands, an effect known as canopy  
428 packing and that has been observed on a variety of mixed forests across Europe

429 (Jucker et al., 2015; Pretzsch, 2019). Here, the mixing effect was tested on  
430 regularized inventories, which means that trees had the same diameter per species  
431 and were regularly spaced. Therefore, only vertical stratification, and no crown  
432 plasticity could emerge in the simulation Jucker et al. (2015).

433 In addition, species mixing increased the yearly water shortage, due to in-  
434 creased transpiration (Figure B.7). This confirms the idea that the nature of  
435 the diversity-functioning relationship in forests strongly depends on the limiting  
436 resources (Forrester, 2014). According to our simulations, promoting diverse  
437 stands could maximize light interception Jucker et al. (2015) but would also in-  
438 crease transpiration, which would be detrimental in water-stressed sites. The use  
439 of an individual-based and process-based model such as PDG-Arena, in combi-  
440 nation with the measurements of physiological traits in mixed stands could help  
441 better understand the relationship between tree diversity, stand productivity and  
442 resistance to water stress.

443 One limit of this study was the nature of the data used to evaluate the model.  
444 Tree growth is an integrative measure that results from carbon, water and light  
445 uptake, whereas CASTANEA is calibrated using CO<sub>2</sub> fluxes, (Dufrêne et al.,  
446 2005). Moreover, the modeling of carbon allocation, which plays a decisive role  
447 in simulating wood growth, can still be improved (Davi et al., 2009; Merganičová  
448 et al., 2019). Additionally, the climate was parameterized at the site scale instead  
449 of the stand scale, although climatic variables such as precipitation could vary  
450 between stands due to local topography.

451 PDG-Arena can be developed further for simulating even more finely inter-  
452 specific interactions. Firstly, the modeling of the soil does not let individual trees  
453 uptake water from different sources whether horizontally or vertically, although

454 this has been proven to occur and be a factor of species differentiation ([Schume](#)  
455 [et al., 2004](#)). Although in our case, the distribution of trees over a small area  
456 (a few meters) may allow us to neglect horizontal heterogeneity, an effort should  
457 be made to differentiate access to the soil water resource according to the state  
458 of the trees (age, size) but also according to interspecific differences. Secondly,  
459 we did not implement phenotypic plasticity, which plays a significant role in the  
460 functioning of mixed forests ([Pretzsch, 2019](#); [Dieler and Pretzsch, 2013](#); [Jucker](#)  
461 [et al., 2015](#)). Thus, our model can only simulate the vertical stratification of  
462 crowns, but not their morphological adaptation to their local competitor (see,  
463 for example, [Jonard et al., 2020](#) and [Morin et al., 2021](#)). Finally, the radiative  
464 model of PDG-Arena does not directly simulate intra-annual variation in light  
465 competition, which could be caused by species differences in leaf phenology.

466 In conclusion, the new individual-based model PDG-Arena we developed can  
467 accurately simulate the interactions between trees in monospecific and mixed  
468 stands and predict their productivity. Compared to CASTANEA, PDG-Arena  
469 showed improved predictive capability for beech and mixed beech-fir forests. As  
470 PDG-Arena simulates the competition for water and light between trees with no  
471 preconceived ideas about the direction of interspecific interaction (from competi-  
472 tion to complementarity), it can be used to test specific hypotheses about mixed  
473 forests and better understand the diversity-functioning relationship in forests un-  
474 der contrasted scenarios. For example, one could explore the following outstand-  
475 ing questions, keeping in mind that the answers are largely dependent on the  
476 species identities ([Ratcliffe et al., 2015](#)) and on each resource scarcity in a given  
477 environment ([Forrester et al., 2017a](#)): is overyielding more likely to occur in less  
478 productive sites? ([Toïgo et al., 2015](#)) Can overyielding increase water stress in

479 mixed stands? (Forrester et al., 2016) Lastly, being made on the basis of a  
480 physio-demo-genetics model, PDG-Arena is suitable to evaluate the evolutionary  
481 dynamics of functional traits under various biotic (stand composition, density  
482 and structure) and abiotic (soil, climate) constraints, as intraspecific diversity is  
483 a major adaptive force in natural tree populations (Lefèvre et al., 2014; Oddou-  
484 Muratorio et al., 2020).

## 485 5. Declarations

### 486 5.1. Declaration of competing interest

487 The authors of this publication declare that they have no conflicts of interest.

### 488 5.2. Funding source

489 This work was financed by ADEME, the French Agency for Ecological Tran-  
490 sition, and ONF, the French National Forests Office. The observation design used  
491 in this study is part of the GMAP network <https://oreme.org/observation/foret/gmap/>,  
492 partly funded by the OSU OREME.

### 493 5.3. Credits

494 Figures 1 and 2 were designed using images from flaticon.com.

### 495 5.4. Author contributions

496 **Camille Rouet**: Conceptualization, Methodology, Software, Visualization,  
497 Writing - Original Draft. **Hendrik Davi**: Conceptualization, Supervision. **Ar-  
498 sène Druel**: Methodology, Writing - Review. **Bruno Fady**: Project admin-  
499 istration, Supervision, Writing - Review. **Xavier Morin**: Methodology, Data  
500 Curation, Supervision, Writing - Review.

## 501 Appendix A. Supplementary description of PDG-Arena

### 502 Appendix A.1. Computing of Leaf Mass per Area

503 The Leaf Mass per Area (LMA) is a key physiological parameter defining the  
504 mass per unit area of leaves ( $\text{g}/\text{m}^2$ ). LMA varies both in time during leaf growth  
505 and in space: leaf mass gain is indeed favored by the light level, resulting in an  
506 exponentially decreasing distribution of LMA across the canopy from top to bot-  
507 tom. In the CASTANEA model, which assumes that the stand is homogeneous  
508 and monospecific, the LMA decay follows an exponential distribution according  
509 to an attenuation coefficient  $kLMA$  for each species:

$$LMA(LAI_{above}) = LMA_0 \times e^{kLMA \times LAI_{above}} \quad (\text{A.1})$$

510  $LAI_{above}$  is given by the position of the considered layer within the canopy.  
511 The average  $LMA$  within a layer is then obtained by integrating  $LMA(LAI_{above})$   
512 within the layer vertical boundaries.  $LMA_0$  and  $kLMA$  depend on the species  
513 and describe the decrease in LMA within the canopy, which itself depends on the  
514 decrease in light intensity within the canopy.

515 In the case of the PDG-Arena model, the canopy is more structurally complex  
516 than in CASTANEA and can include several species with different  $kLMA$ . Then,  
517 the LMA of each crown is defined according to its position within the global  
518 canopy, taking all trees into account and using the same equation as [A.1](#). Here,  
519  $LAI_{above}$  is computed as the sum of the LAI from the different crowns that  
520 are located above the considered layer of leaves. It should be noted that the  
521 model is not completely accurate given that the parameter  $kLMA$  is species-  
522 dependent, although the leaves taken into account in  $LAI_{above}$  potentially come

523 from another species. However, this method does represent the phenomenon of  
524 light attenuation which is specific to each individual.

525 *Appendix A.2. Estimation of the attenuation coefficient with reverse-engineering*

526 In order to know the value of the attenuation coefficients of each species  
527 in PDG-Arena, a preliminary simulation is carried out following the CASTANEA  
528 model to take advantage of the SAIL, its radiation balance sub-model (Dufrêne  
529 et al., 2005). The preliminary simulation is performed for each species on a  
530 monospecific and regularized inventory (RN inventory, see section 2.3). We  
531 define the attenuation coefficient  $k_1$  at a given time as a function of the incident  
532 energy  $I_0$ , the energy transmitted by the vegetation  $I_t$ , and the Leaf Area Index  
533  $LAI$ , following a Beer-Lambert model:

$$I_t = I_0 \exp^{-k_1 \times LAI} \quad (\text{A.2})$$

534 which is equivalent to:

$$k_1 = \frac{1}{LAI} \times \log\left(\frac{I_0}{I_t}\right) \quad (\text{A.3})$$

535 where  $I_t$  is defined at any time as the difference between the incident energy and  
536 the energy absorbed by the vegetation.

537 The coefficient of attenuation which is used in SamsaraLight, denoted  $k_2$ ,  
538 is not of the same nature as  $k_1$ . Indeed, in equation A.2, we multiply  $k_1$  to  
539 the  $LAI$  (considering an infinite, horizontally homogeneous, leaf layer) while  
540 SamsaraLight multiplies  $k_2$  to the Leaf Area Density  $LAD$  and the beam path  
541 length within a finite, volumetric crown (see equation 2). Then, to go from one  
542 to the other, we must multiply  $k_1$  by  $\sin(\beta)$  (with  $\beta$  the angle of height of the

543 sun):

$$k_2 = \sin(\beta) \times k_1 = \sin(\beta) \times \frac{1}{LAI} \times \log\left(\frac{I_0}{I_t}\right) \quad (\text{A.4})$$

544 The coefficient  $k_2$  depends on the height of the sun, but also on the fre-  
545 quency domain of the radiation. Indeed, the attenuation coefficient takes into  
546 account both the extinction of the rays (defined by the leaf and crown geometry)  
547 and the absorption by the leaves which depends on the light frequency. In the  
548 following calculations, we distinguish the PAR (photosynthetically active radia-  
549 tions) domain for which the absorption is maximized and the NIR (near infrared  
550 radiations) domain. It is assumed that these two domains represent the bulk  
551 of the incident radiation. To sum up, the attenuation coefficient depends on  
552 the species (leaf angle distribution and absorbance rate), the type of radiation  
553 (PAR/NIR, direct/diffuse) and the height angle ( $\beta$ ).

554 Based on the results of the preliminary CASTANEA simulation, which exe-  
555 cutes a radiation balance using the SAIL model, we infer the value of the atten-  
556 uation coefficients of the plot for direct and diffuse radiations. In the preliminary  
557 simulation, we know for direct rays the value of the height angle  $\beta$  at any hour.  
558 For diffuse rays, by definition  $\beta$  takes every value between 0 and  $\pi/2$  at any hour,  
559 so we can't use the height angle information.

560 *Direct Rays.*

561 For direct radiation, we estimate an attenuation coefficient for each species by  
562 discriminating the PAR and NIR and defining 20 classes of attenuation coefficient  
563 corresponding to classes of height angle  $\beta$ , equally distributed between 0 and  $\pi/2$ .  
564 For each  $i$  class of  $\beta$ , we performed an average on the attenuation coefficients



565 observed during the preliminary simulation for direct radiations:

$$k_{dir}(i) = \sum_{h_i} \left[ \sin(\beta(h_i)) \times \frac{1}{LAI(h_i)} \times \log\left(\frac{I_{0dir}(h_i)}{I_{tdir}(h_i)}\right) \right] \times \frac{1}{n(h_i)} \quad (\text{A.5})$$

566  $k_{dir}(i)$  is the mean attenuation coefficient computed from the preliminary  
567 simulation results, for direct radiation of the height angle class  $i$  (which includes  
568  $n(h_i)$  hours). For a given hour of the year  $h_i$  and sun angle  $\beta(h_i)$ ,  $LAI(h_i)$  is  
569 the daily Leaf Area Index of the plot,  $I_{0dir}(h_i)$ , the incident direct energy and  
570  $I_{tdir}(h_i)$  is the direct energy transmitted through canopy.

571 *Diffuse Radiation.*

572 For diffuse radiation, we discriminate the attenuation coefficient according  
573 to the species and radiation domain only. The attenuation coefficient for diffuse  
574 light  $k_{dif}$  is assumed to be constant for any sun height angle. To switch from  
575 one formulation of the Beer-Lambert law to the other (equation A.4), a value of  
576  $\beta$  is nevertheless needed. We note that the distribution of the diffuse rays along  
577 the  $\beta$  height angles is uniform. Then, we use  $\overline{\sin(\beta)}$ , the average of  $\sin(\beta)$  for  
578  $\beta$  going from 0 to  $\pi/2$  (which is about 0.637). For a species and a radiative  
579 domain, we compute an average on every day of year of the observed attenuation  
580 coefficient during the preliminary simulation:

$$k_{dif} = \sum_j \left[ \overline{\sin(\beta)} \times \frac{1}{LAI(j)} \times \log\left(\frac{I_{0dif}(j)}{I_{tdif}(j)}\right) \right] \times \frac{1}{365} \quad (\text{A.6})$$

581 with, for the day  $j$ ,  $LAI(j)$  the Leaf Area Index,  $I_{0dif}(j)$  the incident diffuse  
582 energy and  $I_{tdif}(j)$  is the diffuse energy transmitted through canopy.

583 *Appendix A.3. Distribution of radiations into canopy layers and into sun and*  
584 *shade leaves*

585 In CASTANEA, the energy absorbed by the canopy is distributed into five  
586 layers of leaves, which are themselves divided into leaves in direct light (called  
587 sun leaves) and leaves in the shade. We present here how PDG-Arena operates  
588 the distribution of the absorbed energy by individual crowns.

589 *Proportion of sun leaves of a tree.*

590 The proportion of sun leaves of a crown, i.e., of its leaves subjected to direct  
591 radiation, is given by a formula borrowed from the HETEROFOR model ([Jonard  
592 et al., 2020](#)). Two factors define the shading received by the leaves of a tree:  
593 on the one hand, the external shading provided by the competing trees, given by  
594 the proportion  $pSun_{ext}$ ; on the other hand, the internal shading provided by the  
595 own leaves of a tree, given by the proportion  $pSun_{int}$ .

596 The shading provided by the competitors is given by the ratio of the direct  
597 energy incident on the tree  $I_{d0}(aboveTree)$  to the direct energy incident on the  
598 stand  $I_{d0}(aboveCanopy)$ :

$$pSun_{ext} = \frac{I_{d0}(aboveTree)}{I_{d0}(aboveCanopy)} \quad (A.7)$$

599 The second quotient to be evaluated is the proportion of the tree's leaves  
600 shaded by its own leaves. The shading by the leaves of the tree itself follows  
601 the same evolution as the direct radiation within the tree, that is to say a Beer-  
602 Lambert law:

$$pSun(l) = p(0) \times \exp^{-k_{dir}l} \quad (A.8)$$

603 where  $pSun(l)$  is the proportion of sun leaves remaining after the radiation

604 passes through the crown, with  $l$  the cumulative LAI encountered by the passing  
605 beam and  $k_{dir}$  the tree extinction coefficient for direct PAR.  $p(0) = 1$  is the pro-  
606 portion of sun leaves at the crown entrance ignoring leaves shaded by neighboring  
607 trees.

608 We can compute  $LAI_{sun-int}$ , the amount of leaves that are not shaded by  
609 leaves of the same tree. To do this, we need to integrate  $p(l)$  for  $l$  ranging from  
610 0 to  $LAI$ , the Leaf Area Index of the tree:

$$\begin{aligned} LAI_{sun-int} &= \int_0^{LAI} p(l) dl \\ &= \int_0^{LAI} e^{-k_{dir}l} dl \\ &= \left[ \frac{e^{-k_{dir}l}}{-k_{dir}} \right]_0^{LAI} \\ &= \frac{1 - e^{-k_{dir}LAI}}{k_{dir}} \end{aligned} \tag{A.9}$$

611 Thus,  $pSun_{int} = LAI_{sun-int}/LAI$  represents the proportion of leaf remain-  
612 ing in the light when shaded by the tree's own leaves.

613 Finally, the proportion of sun leaves of a tree is  $pSun_{tree} = pSun_{ext} \times$   
614  $pSun_{int}$ .

615

616 *Distribution of radiations by layer.*

617 If SamsaraLight allows us to know the amount of energy absorbed per tree  
618 according to each domain (PAR/NIR) and type of energy (direct/diffused), noted  
619  $E_{tree}$ , it does not allow us to distribute this amount between layers, differentiating  
620 leaves with high interception and leaves with low interception. Firstly, we divide  
621 the leaf surface of a tree in  $n$  equal-sized layers, and we assume that the radiative

622 characteristics are homogeneous within a layer. We define a distribution function  
623  $f_i$ , that determines  $E_i$ , the amount of energy that is absorbed from layer  $i$ :

$$E_i = E_{tree} \times \frac{f_i}{\sum_n f_i} \quad (\text{A.10})$$

624 We assume that the distribution  $f_i$  is affected by the light interception from  
625 leaf surface that is located above the layer (whether it belongs to other trees or  
626 to the same tree). Then, we define a simple stand-scale model that describes  
627 the level of energy transmitted through the stand using a Beer-Lambert law. At  
628 any level of height located under a quantity of leaves  $LAI_{above}$ , the proportion  
629 of light transmitted through these leaves is:

$$p_{light}(LAI_{above}) = e^{-k_{st} \times LAI_{above}} \quad (\text{A.11})$$

630 with  $k_{st}$  the stand level attenuation coefficient.  $LAI_{above}$  is calculated by  
631 counting the amount of leaves above the leaf layer under consideration, knowing  
632 the position and shape of each individual. A homogeneous distribution of leaf  
633 density within each individual crown is assumed. We do not consider the slope  
634 in this calculation, i.e., only the height of the trees defines whether the leaves of  
635 one tree are higher than those of another.

636 Finally, to calculate  $f_i$ , the fraction of energy absorbed by any layer  $i$  of a  
637 crown, we compute the average value of  $p_{light}$  inside the layer by integrating it  
638 within its boundaries  $LAI_{above}(i - 1)$  and  $LAI_{above}(i)$ :

$$\begin{aligned}
 f_i &= \frac{\int_{LAI_{above}(i-1)}^{LAI_{above}(i)} e^{-k_{st}LAI_{above}} dLAI_{above}}{LAI_{above}(i) - LAI_{above}(i-1)} \\
 &\iff \\
 f_i &= \frac{e^{-k_{st}LAI_{above}(i-1)} - e^{-k_{st}LAI_{above}(i)}}{k_{st}(LAI_{above}(i) - LAI_{above}(i-1))}
 \end{aligned} \tag{A.12}$$

639 The proportion  $f_i$  is computed for each type of radiation (direct/diffuse and  
 640 PAR/NIR).

641

#### 642 *Appendix A.4. Reduction of absorbed radiations in SamsaraLight*

643 In SamsaraLight standard mode, the foliage is assumed to be at its maximum  
 644 during the whole process. Thus, the energy absorbed by the trees when their leaf  
 645 area is in reality lower must be revised downwards, especially for deciduous trees,  
 646 which lose all their foliage in autumn. For each individual, a ratio depending on  
 647 its LAI is computed each day to represent the evolution of its absorption level  
 648 from 0 to 1. The level of absorption is supposed to follow the dynamic of the  
 649 Beer-Lambert law:

$$ratio_{LAI} = \frac{1 - e^{-k \times LAI}}{1 - e^{-k \times LAI_{max}}} \tag{A.13}$$

650 For each radiation domain,  $k$  is the attenuation coefficient of a tree and  
 651  $ratio_{LAI}$  is applied to its absorbed energy to take off the surplus. Neverthe-  
 652 less, the removed energy must be redistributed, because if it had not been in-  
 653 tercepted, this energy would have been distributed among the other absorbing  
 654 elements (crowns or soil cells). At this point, it is no longer possible to know to  
 655 which element the energy should be distributed. Then, the extracted energy is

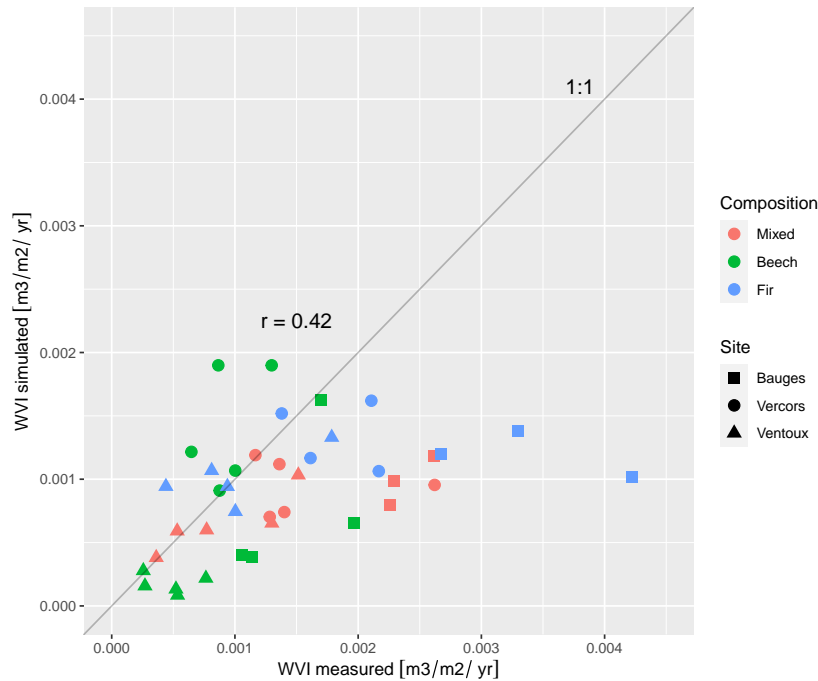


Figure B.5: Simulated versus measured Wood Volume Increment per stand for the CASTANEA model.  $r$  is the correlation coefficient.

656 redistributed to all absorbing elements, proportionally to their level of absorbed  
657 energy (after reduction according to LAI), which represents their relative inter-  
658 ception capacity.

## 659 Appendix B. Supplementary figures

660 Figures B.5 and B.6 show the simulated versus measured wood volume in-  
661 crement per stand for the 39 stands using the CASTANEA model and the PDG-  
662 Arena model (with O inventories), respectively.

663 Figure B.7 shows the maximum water shortage during an average year (i.e.  
664 the maximum difference reached during a year between the current and full useful  
665 reserve, in mm) and yearly transpiration simulated by PDG-Arena for 13 mixed

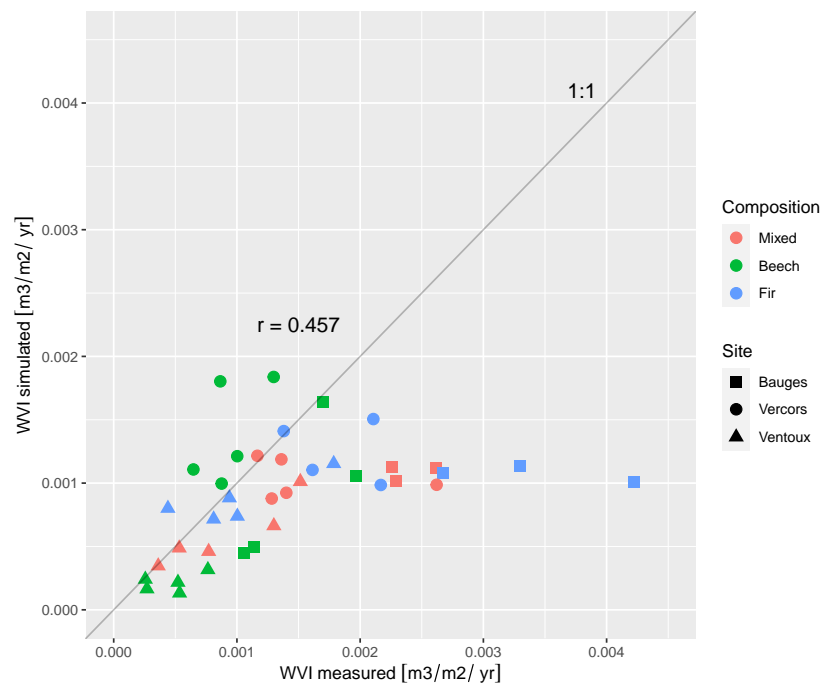


Figure B.6: Simulated versus measured Wood Volume Increment per stand for the PDG-Arena model using original inventories.  $r$  is the correlation coefficient.

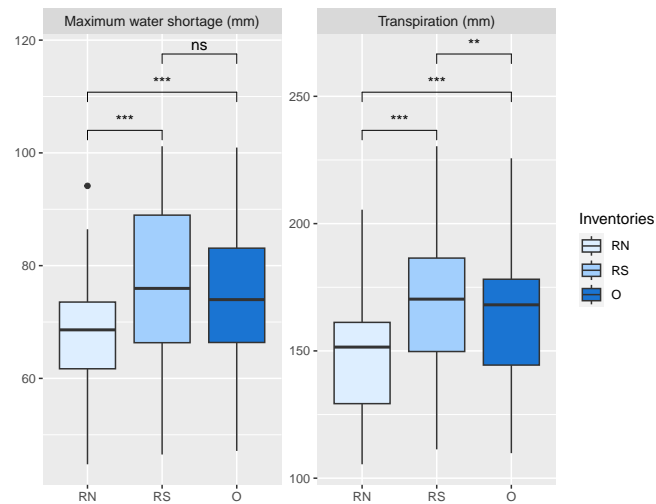


Figure B.7: Maximum water shortage during an average year and yearly transpiration simulated by PDG-Arena for 13 mixed stands. Three types of inventories were used: regularized inventories with no species interactions (RN), regularized inventories with species interactions (RS) and original inventories (O). Two-sided Wilcoxon signed rank test was used (\*\*\*: p-value < 0.001).

666 stands using RN, RS and O inventories.



## References

- Ammer, C., 2019. Diversity and forest productivity in a changing climate. *New Phytologist* 221, 50–66. doi:[10.1111/nph.15263](https://doi.org/10.1111/nph.15263).
- Bauhus, J., Forrester, D.I., Pretzsch, H., 2017. From Observations to Evidence About Effects of Mixed-Species Stands, in: Pretzsch, H., Forrester, D.I., Bauhus, J. (Eds.), *Mixed-Species Forests: Ecology and Management*. Springer, Berlin, Heidelberg, pp. 27–71. doi:[10.1007/978-3-662-54553-9\\_2](https://doi.org/10.1007/978-3-662-54553-9_2).
- Bonan, G.B., 2008. Forests and Climate Change: Forcings, Feedbacks, and the Climate Benefits of Forests. *Science* 320, 1444–1449. doi:[10.1126/science.1155121](https://doi.org/10.1126/science.1155121).
- Cordonnier, T., Smadi, C., Kunstler, G., Courbaud, B., 2019. Asymmetric competition, ontogenetic growth and size inequality drive the difference in productivity between two-strata and one-stratum forest stands. *Theoretical Population Biology* 130, 83–93. doi:[10.1016/j.tpb.2019.07.001](https://doi.org/10.1016/j.tpb.2019.07.001).
- Courbaud, B., de Coligny, F., Cordonnier, T., 2003. Simulating radiation distribution in a heterogeneous Norway spruce forest on a slope. *Agricultural and Forest Meteorology* 116, 1–18. doi:[10.1016/S0168-1923\(02\)00254-X](https://doi.org/10.1016/S0168-1923(02)00254-X).
- Cuddington, K., Fortin, M.J., Gerber, L.R., Hastings, A., Liebhold, A., O'Connor, M., Ray, C., 2013. Process-based models are required to manage ecological systems in a changing world. *Ecosphere* 4, art20. doi:[10.1890/ES12-00178.1](https://doi.org/10.1890/ES12-00178.1).
- Davi, H., Barbaroux, C., Dufrêne, E., François, C., Montpied, P., Bréda, N., Badeck, F., 2008a. Modelling leaf mass per area in forest canopy as affected by prevailing radiation conditions. *Ecological Modelling* 211, 339–349. doi:[10.1016/j.ecolmodel.2007.09.012](https://doi.org/10.1016/j.ecolmodel.2007.09.012).
- Davi, H., Barbaroux, C., Francois, C., Dufrêne, E., 2009. The fundamental role of reserves and hydraulic constraints in predicting LAI and carbon allocation in forests. *Agricultural and Forest Meteorology* 149, 349–361. doi:[10.1016/j.agrformet.2008.08.014](https://doi.org/10.1016/j.agrformet.2008.08.014).
- Davi, H., Baret, F., Huc, R., Dufrêne, E., 2008b. Effect of thinning on LAI variance in heterogeneous forests. *Forest Ecology and Management* 256, 890–899. doi:[10.1016/j.foreco.2008.05.047](https://doi.org/10.1016/j.foreco.2008.05.047).
- Davi, H., Cailleret, M., 2017. Assessing drought-driven mortality trees with physiological process-based models. *Agricultural and Forest Meteorology* 232, 279–290. doi:[10.1016/j.agrformet.2016.08.019](https://doi.org/10.1016/j.agrformet.2016.08.019).

- Dieler, J., Pretzsch, H., 2013. Morphological plasticity of European beech (*Fagus sylvatica* L.) in pure and mixed-species stands. *Forest Ecology and Management* 295, 97–108. doi:[10.1016/j.foreco.2012.12.049](https://doi.org/10.1016/j.foreco.2012.12.049).
- Dufour-Kowalski, S., Courbaud, B., Dreyfus, P., Meredieu, C., de Coligny, F., 2012. Capsis: an open software framework and community for forest growth modelling. *Annals of Forest Science* 69, 221–233. doi:[10.1007/s13595-011-0140-9](https://doi.org/10.1007/s13595-011-0140-9).
- Dufrêne, E., Davi, H., François, C., Maire, G.I., Dantec, V.L., Granier, A., 2005. Modelling carbon and water cycles in a beech forest. Part I: Model description and uncertainty analysis on modelled NEE. *Ecological Modelling* 185, 407–436. doi:[10/fjnfgr](https://doi.org/10/fjnfgr).
- Dănescu, A., Albrecht, A.T., Bauhus, J., 2016. Structural diversity promotes productivity of mixed, uneven-aged forests in southwestern Germany. *Oecologia* 182, 319–333. doi:[10.1007/s00442-016-3623-4](https://doi.org/10.1007/s00442-016-3623-4).
- Fontes, L., Bontemps, J.D., Bugmann, H., Oijen, M.v., Gracia, C., Kramer, K., Lindner, M., Rötzer, T., Skovsgaard, J.P., 2010. Models for supporting forest management in a changing environment. *Forest Systems* 19, 8–29.
- Forrester, D.I., 2014. The spatial and temporal dynamics of species interactions in mixed-species forests: From pattern to process. *Forest Ecology and Management* 312, 282–292. doi:[10.1016/j.foreco.2013.10.003](https://doi.org/10.1016/j.foreco.2013.10.003).
- Forrester, D.I., Ammer, C., Annighöfer, P.J., Avdagic, A., Barbeito, I., Bielak, K., Brazaitis, G., Coll, L., del Río, M., Drössler, L., Heym, M., Hurt, V., Löf, M., Matović, B., Meloni, F., den Ouden, J., Pach, M., Pereira, M.G., Ponette, Q., Pretzsch, H., Skrzyszewski, J., Stojanović, D., Svoboda, M., Ruiz-Peinado, R., Vacciano, G., Verheyen, K., Zlatanov, T., Bravo-Oviedo, A., 2017a. Predicting the spatial and temporal dynamics of species interactions in *Fagus sylvatica* and *Pinus sylvestris* forests across Europe. *Forest Ecology and Management* 405, 112–133. doi:[10.1016/j.foreco.2017.09.029](https://doi.org/10.1016/j.foreco.2017.09.029).
- Forrester, D.I., Bauhus, J., 2016. A Review of Processes Behind Diversity—Productivity Relationships in Forests. *Current Forestry Reports* 2, 45–61. doi:[10.1007/s40725-016-0031-2](https://doi.org/10.1007/s40725-016-0031-2).
- Forrester, D.I., Bonal, D., Dawud, S., Gessler, A., Granier, A., Pollastrini, M., Grossiord, C., 2016. Drought responses by individual tree species are not often correlated with tree species diversity in European forests. *Journal of Applied Ecology* 53, 1725–1734. doi:[10.1111/1365-2664.12745](https://doi.org/10.1111/1365-2664.12745).

- Forrester, D.I., Tachauer, I.H.H., Annighoefer, P., Barbeito, I., Pretzsch, H., Ruiz-Peinado, R., Stark, H., Vacchiano, G., Zlatanov, T., Chakraborty, T., Saha, S., Sileshi, G.W., 2017b. Generalized biomass and leaf area allometric equations for European tree species incorporating stand structure, tree age and climate. *Forest Ecology and Management* 396, 160–175. doi:[10.1016/j.foreco.2017.04.011](https://doi.org/10.1016/j.foreco.2017.04.011).
- Gonçalves, A.F.A., Santos, J.A.d., França, L.C.d.J., Campoe, O.C., Altoé, T.F., Scolforo, J.R.S., 2021. Use of the process-based models in forest research: a bibliometric review. *CERNE* 27, e. doi:[10.1590/01047760202127012769](https://doi.org/10.1590/01047760202127012769).
- Grossiord, C., 2018. Having the right neighbors: how tree species diversity modulates drought impacts on forests. *New Phytologist* 228, 42–49. doi:<https://doi.org/10.1111/nph.15667>.
- Grossiord, C., Granier, A., Ratcliffe, S., Bouriaud, O., Bruelheide, H., Čečko, E., Forrester, D.I., Dawud, S.M., Finér, L., Pollastrini, M., Scherer-Lorenzen, M., Valadares, F., Bonal, D., Gessler, A., 2014. Tree diversity does not always improve resistance of forest ecosystems to drought. *Proceedings of the National Academy of Sciences* 111, 14812–14815. doi:[10.1073/pnas.1411970111](https://doi.org/10.1073/pnas.1411970111).
- Guillemot, J., Kunz, M., Schnabel, F., Fichtner, A., Madsen, C.P., Gebauer, T., Härdtle, W., von Oheimb, G., Potvin, C., 2020. Neighbourhood-mediated shifts in tree biomass allocation drive overyielding in tropical species mixtures. *New Phytologist* 228, 1256–1268. doi:[10.1111/nph.16722](https://doi.org/10.1111/nph.16722).
- Jonard, M., André, F., de Coligny, F., de Wergifosse, L., Beudez, N., Davi, H., Ligot, G., Ponette, Q., Vincke, C., 2020. HETEROFOR 1.0: a spatially explicit model for exploring the response of structurally complex forests to uncertain future conditions – Part 1: Carbon fluxes and tree dimensional growth. *Geoscientific Model Development* 13, 905–935. doi:[10.5194/gmd-13-905-2020](https://doi.org/10.5194/gmd-13-905-2020).
- Jourdan, M., Cordonnier, T., Dreyfus, P., Rioud, C., de Coligny, F., Morin, X., 2021. Managing mixed stands can mitigate severe climate change impacts on French alpine forests. *Regional Environmental Change* 21, 78. doi:[10.1007/s10113-021-01805-y](https://doi.org/10.1007/s10113-021-01805-y).
- Jourdan, M., Kunstler, G., Morin, X., 2020. How neighbourhood interactions control the temporal stability and resilience to drought of trees in mountain forests. *Journal of Ecology* 108, 666–677. doi:<https://doi.org/10.1111/1365-2745.13294>.

- Jourdan, M., Lebourgeois, F., Morin, X., 2019. The effect of tree diversity on the resistance and recovery of forest stands in the French Alps may depend on species differences in hydraulic features. *Forest Ecology and Management* 450, 117486. doi:[10.1016/j.foreco.2019.117486](https://doi.org/10.1016/j.foreco.2019.117486).
- Jucker, T., Bouriaud, O., Avacaritei, D., Dănilă, I., Duduman, G., Valladares, F., Coomes, D.A., 2014. Competition for light and water play contrasting roles in driving diversity-productivity relationships in Iberian forests. *Journal of Ecology* 102, 1202–1213. doi:[10.1111/1365-2745.12276](https://doi.org/10.1111/1365-2745.12276).
- Jucker, T., Bouriaud, O., Coomes, D.A., 2015. Crown plasticity enables trees to optimize canopy packing in mixed-species forests. *Functional Ecology* 29, 1078–1086. doi:[10.1111/1365-2435.12428](https://doi.org/10.1111/1365-2435.12428).
- Korzukhin, M.D., Ter-Mikaelian, M.T., Wagner, R.G., 1996. Process versus empirical models: which approach for forest ecosystem management? *Canadian Journal of Forest Research* 26, 879–887. doi:[10.1139/x26-096](https://doi.org/10.1139/x26-096).
- Lefèvre, F., Boivin, T., Bontemps, A., Courbet, F., Davi, H., Durand-Gillmann, M., Fady, B., Gauzere, J., Gidoïn, C., Karam, M.J., Lalagüe, H., Oddou-Muratorio, S., Pichot, C., 2014. Considering evolutionary processes in adaptive forestry. *Annals of Forest Science* 71, 723–739. doi:[10.1007/s13595-013-0272-1](https://doi.org/10.1007/s13595-013-0272-1).
- Leuning, R., Kelliher, F.M., Pury, D.G.G.D., Schulze, E.D., 1995. Leaf nitrogen, photosynthesis, conductance and transpiration: scaling from leaves to canopies. *Plant, Cell & Environment* 18, 1183–1200. doi:<https://doi.org/10.1111/j.1365-3040.1995.tb00628.x>.
- Liang, J., Crowther, T.W., Picard, N., Wiser, S., Zhou, M., Alberti, G., Schulze, E.D., McGuire, A.D., Bozzato, F., Pretzsch, H., de Miguel, S., Paquette, A., Hérault, B., Scherer-Lorenzen, M., Barrett, C.B., Glick, H.B., Hengeveld, G.M., Nabuurs, G.J., Pfautsch, S., Viana, H., Vibrans, A.C., Ammer, C., Schall, P., Verbyla, D., Tchebakova, N., Fischer, M., Watson, J.V., Chen, H.Y.H., Lei, X., Schelhaas, M.J., Lu, H., Gianelle, D., Parfenova, E.I., Salas, C., Lee, E., Lee, B., Kim, H.S., Bruelheide, H., Coomes, D.A., Piotta, D., Sunderland, T., Schmid, B., Gourlet-Fleury, S., Sonké, B., Tavana, R., Zhu, J., Brandl, S., Vayreda, J., Kitahara, F., Searle, E.B., Neldner, V.J., Ngugi, M.R., Baraloto, C., Frizzera, L., Bałazy, R., Oleksyn, J., Zawila-Niedzwiecki, T., Bouriaud, O., Bussotti, F., Finér, L., Jaroszewicz, B., Jucker, T., Valladares, F., Jagodzinski, A.M., Peri, P.L., Gonmadje, C., Marthy, W., O'Brien, T., Martin, E.H., Marshall, A.R., Rovero, F., Bitariho, R., Niklaus, P.A., Alvarez-Loayza, P., Chamuya, N., Valencia, R., Mortier, F., Wortel, V., Engone-Obiang, N.L., Ferreira, L.V., Odeke, D.E., Vasquez, R.M., Lewis, S.L., Reich, P.B.,

2016. Positive biodiversity-productivity relationship predominant in global forests. *Science* 354. doi:[10.1126/science.aaf8957](https://doi.org/10.1126/science.aaf8957).
- Lindner, M., Maroschek, M., Netherer, S., Kremer, A., Barbati, A., Garcia-Gonzalo, J., Seidl, R., Delzon, S., Corona, P., Kolström, M., Lexer, M.J., Marchetti, M., 2010. Climate change impacts, adaptive capacity, and vulnerability of European forest ecosystems. *Forest Ecology and Management* 259, 698–709. doi:[10.1016/j.foreco.2009.09.023](https://doi.org/10.1016/j.foreco.2009.09.023).
- Loreau, M., 2010. CHAPTER 3. Biodiversity and Ecosystem Functioning, in: *From Populations to Ecosystems*. Princeton University Press, pp. 56–78. doi:[10.1515/9781400834167.56](https://doi.org/10.1515/9781400834167.56).
- Mas, E., Cochard, H., Deluigi, J., Didion-Gency, M., Martin-StPaul, N., Morcillo, L., Valladares, F., Vilagrosa, A., Grossiord, C., 2024. Interactions between beech and oak seedlings can modify the effects of hotter droughts and the onset of hydraulic failure. *New Phytologist* 241, 1021–1034. doi:[10.1111/nph.19358](https://doi.org/10.1111/nph.19358).
- Merganičová, K., Merganič, J., Lehtonen, A., Vacchiano, G., Sever, M.Z.O., Augustynczyk, A.L.D., Grote, R., Kyselová, I., Mäkelä, A., Yousefpour, R., Krejza, J., Collalti, A., Reyer, C.P.O., 2019. Forest carbon allocation modelling under climate change. *Tree Physiology* 39, 1937–1960. doi:[10/ghkr6m](https://doi.org/10/ghkr6m).
- Messier, C., Bauhus, J., Sousa-Silva, R., Auge, H., Baeten, L., Barsoum, N., Bruelheide, H., Caldwell, B., Cavender-Bares, J., Dhiedt, E., Eisenhauer, N., Ganade, G., Gravel, D., Guillemot, J., Hall, J.S., Hector, A., Hérault, B., Jactel, H., Koricheva, J., Kreft, H., Mereu, S., Muys, B., Nock, C.A., Paquette, A., Parker, J.D., Perring, M.P., Ponette, Q., Potvin, C., Reich, P.B., Scherer-Lorenzen, M., Schnabel, F., Verheyen, K., Weih, M., Wollni, M., Zemp, D.C., 2022. For the sake of resilience and multifunctionality, let's diversify planted forests! *Conservation Letters* 15, e12829. doi:[10.1111/conl.12829](https://doi.org/10.1111/conl.12829).
- Metz, J., Annighöfer, P., Schall, P., Zimmermann, J., Kahl, T., Schulze, E.D., Ammer, C., 2016. Site-adapted admixed tree species reduce drought susceptibility of mature European beech. *Global Change Biology* 22, 903–920. doi:[10.1111/gcb.13113](https://doi.org/10.1111/gcb.13113).
- Monteith, J., 1965. Evaporation and environment. *Symposia of the Society for Experimental Biology* .
- Morin, X., Bugmann, H., de Coligny, F., Martin-StPaul, N., Cailleret, M., Limousin, J.M., Ourcival, J.M., Prevosto, B., Simioni, G., Toigo, M., Vennetier, M., Catteau,

- E., Guillemot, J., 2021. Beyond forest succession: A gap model to study ecosystem functioning and tree community composition under climate change. *Functional Ecology* 35, 955–975. doi:[10.1111/1365-2435.13760](https://doi.org/10.1111/1365-2435.13760).
- Morin, X., Fahse, L., de Mazancourt, C., Scherer-Lorenzen, M., Bugmann, H., 2014. Temporal stability in forest productivity increases with tree diversity due to asynchrony in species dynamics. *Ecology Letters* 17, 1526–1535. doi:[10.1111/ele.12357](https://doi.org/10.1111/ele.12357).
- Morin, X., Fahse, L., Scherer-Lorenzen, M., Bugmann, H., 2011. Tree species richness promotes productivity in temperate forests through strong complementarity between species: Species richness promotes forest productivity. *Ecology Letters* 14, 1211–1219. doi:[10.1111/j.1461-0248.2011.01691.x](https://doi.org/10.1111/j.1461-0248.2011.01691.x).
- Oddou-Muratorio, S., Davi, H., Lefèvre, F., 2020. Integrating evolutionary, demographic and ecophysiological processes to predict the adaptive dynamics of forest tree populations under global change. *Tree Genetics & Genomes* 16, 67. doi:[10.1007/s11295-020-01451-1](https://doi.org/10.1007/s11295-020-01451-1).
- Oddou-Muratorio, S., Davi, H., 2014. Simulating local adaptation to climate of forest trees with a Physio-Demo-Genetics model. *Evolutionary Applications* 7, 453–467. doi:[10.1111/eva.12143](https://doi.org/10.1111/eva.12143).
- Pardos, M., del Río, M., Pretzsch, H., Jactel, H., Bielak, K., Bravo, F., Brazaitis, G., Defosse, E., Engel, M., Godvod, K., Jacobs, K., Jansone, L., Jansons, A., Morin, X., Nothdurft, A., Oreti, L., Ponette, Q., Pach, M., Riofrío, J., Ruíz-Peinado, R., Tomao, A., Uhl, E., Calama, R., 2021. The greater resilience of mixed forests to drought mainly depends on their composition: Analysis along a climate gradient across Europe. *Forest Ecology and Management* 481, 118687. doi:[10.1016/j.foreco.2020.118687](https://doi.org/10.1016/j.foreco.2020.118687).
- Piotto, D., 2008. A meta-analysis comparing tree growth in monocultures and mixed plantations. *Forest Ecology and Management* 255, 781–786. doi:[10.1016/j.foreco.2007.09.065](https://doi.org/10.1016/j.foreco.2007.09.065).
- van der Plas, F., Manning, P., Allan, E., Scherer-Lorenzen, M., Verheyen, K., Wirth, C., Zavala, M.A., Hector, A., Ampoorter, E., Baeten, L., Barbaro, L., Bauhus, J., Benavides, R., Benneter, A., Berthold, F., Bonal, D., Bouriaud, O., Bruelheide, H., Bussotti, F., Carnol, M., Castagneyrol, B., Charbonnier, Y., Coomes, D., Coppi, A., Bastias, C.C., Muhie Dawud, S., De Wandeler, H., Domisch, T., Finér, L., Gessler, A., Granier, A., Grossiord, C., Guyot, V., Hättenschwiler, S., Jactel, H., Jaroszewicz, B., Joly, F.X., Jucker, T., Koricheva, J., Milligan, H., Müller, S., Muys,

- B., Nguyen, D., Pollastrini, M., Raulund-Rasmussen, K., Selvi, F., Stenlid, J., Valldares, F., Vesterdal, L., Zielinski, D., Fischer, M., 2016. Jack-of-all-trades effects drive biodiversity–ecosystem multifunctionality relationships in European forests. *Nature Communications* 7, 11109. doi:[10.1038/ncomms11109](https://doi.org/10.1038/ncomms11109).
- Porté, A., Bartelink, H.H., 2002. Modelling mixed forest growth: a review of models for forest management. *Ecological Modelling* 150, 141–188. doi:[10.1016/S0304-3800\(01\)00476-8](https://doi.org/10.1016/S0304-3800(01)00476-8).
- Pretzsch, H., 2019. The Effect of Tree Crown Allometry on Community Dynamics in Mixed-Species Stands versus Monocultures. A Review and Perspectives for Modeling and Silvicultural Regulation. *Forests* 10, 810. doi:[10.3390/f10090810](https://doi.org/10.3390/f10090810).
- Pretzsch, H., Forrester, D.I., Bauhus, J. (Eds.), 2017. *Mixed-species forests : ecology and management*. Springer, Berlin.
- Pretzsch, H., Forrester, D.I., Rötzer, T., 2015. Representation of species mixing in forest growth models. A review and perspective. *Ecological Modelling* 313, 276–292. doi:[10.1016/j.ecolmodel.2015.06.044](https://doi.org/10.1016/j.ecolmodel.2015.06.044).
- Pretzsch, H., Schütze, G., Uhl, E., 2013. Resistance of European tree species to drought stress in mixed versus pure forests: evidence of stress release by inter-specific facilitation. *Plant Biology* 15, 483–495. doi:<https://doi.org/10.1111/j.1438-8677.2012.00670.x>.
- Rakovec, O., Samaniego, L., Hari, V., Markonis, Y., Moravec, V., Thober, S., Hanel, M., Kumar, R., 2022. The 2018–2020 Multi-Year Drought Sets a New Benchmark in Europe. *Earth's Future* 10, e2021EF002394. doi:[10.1029/2021EF002394](https://doi.org/10.1029/2021EF002394).
- Ratcliffe, S., Holzwarth, F., Nadrowski, K., Levick, S., Wirth, C., 2015. Tree neighbourhood matters – Tree species composition drives diversity–productivity patterns in a near-natural beech forest. *Forest Ecology and Management* 335, 225–234. doi:[10.1016/j.foreco.2014.09.032](https://doi.org/10.1016/j.foreco.2014.09.032).
- Ratcliffe, S., Liebergesell, M., Ruiz-Benito, P., González, J.M., Castañeda, J.M.M., Kändler, G., Lehtonen, A., Dahlgren, J., Kattge, J., Peñuelas, J., Zavala, M.A., Wirth, C., 2016. Modes of functional biodiversity control on tree productivity across the European continent. *Global Ecology and Biogeography* 25, 251–262. doi:<https://doi.org/10.1111/geb.12406>.
- Reyer, C., 2015. Forest Productivity Under Environmental Change—a Review of Stand-Scale Modeling Studies. *Current Forestry Reports* 1, 53–68. doi:[10.1007/s40725-015-0009-5](https://doi.org/10.1007/s40725-015-0009-5).

- Rolland, C., 2003. Spatial and Seasonal Variations of Air Temperature Lapse Rates in Alpine Regions. *Journal of Climate* 16, 1032–1046. doi:[10.1175/1520-0442\(2003\)016<1032:SASVOA>2.0.CO;2](https://doi.org/10.1175/1520-0442(2003)016<1032:SASVOA>2.0.CO;2).
- Rouet, C., 2024. Data from: PDG-Arena: An ecophysiological model for characterizing tree-tree interactions in heterogeneous stands (v1.0.0). Zenodo. doi:[10.5281/zenodo.10641151](https://doi.org/10.5281/zenodo.10641151).
- del Río, M., Pretzsch, H., Ruiz-Peinado, R., Jactel, H., Coll, L., Löf, M., Aldea, J., Ammer, C., Avdagić, A., Barbeito, I., Bielak, K., Bravo, F., Brazaitis, G., Cerný, J., Collet, C., Condés, S., Drössler, L., Fabrika, M., Heym, M., Holm, S.O., Hylen, G., Jansons, A., Kurylyak, V., Lombardi, F., Matović, B., Metslaid, M., Motta, R., Nord-Larsen, T., Nothdurft, A., den Ouden, J., Pach, M., Pardos, M., Poeydebat, C., Ponette, Q., Pérot, T., Reventlow, D.O.J., Sitko, R., Sramek, V., Steckel, M., Svoboda, M., Verheyen, K., Vospernik, S., Wolff, B., Zlatanov, T., Bravo-Oviedo, A., 2022. Emerging stability of forest productivity by mixing two species buffers temperature destabilizing effect. *Journal of Applied Ecology* 59, 2730–2741. doi:[10.1111/1365-2664.14267](https://doi.org/10.1111/1365-2664.14267).
- Schume, H., Jost, G., Hager, H., 2004. Soil water depletion and recharge patterns in mixed and pure forest stands of European beech and Norway spruce. *Journal of Hydrology* 289, 258–274. doi:[10.1016/j.jhydrol.2003.11.036](https://doi.org/10.1016/j.jhydrol.2003.11.036).
- Seynave, I., Bailly, A., Balandier, P., Bontemps, J.D., Cailly, P., Cordonnier, T., Deleuze, C., Dhôte, J.F., Ginisty, C., Lebourgeois, F., Merzeau, D., Paillassa, E., Perret, S., Richter, C., Meredieu, C., 2018. GIS Coop: networks of silvicultural trials for supporting forest management under changing environment. *Annals of Forest Science* 75, 1–20. doi:[10.1007/s13595-018-0692-z](https://doi.org/10.1007/s13595-018-0692-z).
- Toïgo, M., Vallet, P., Perot, T., Bontemps, J.D., Piedallu, C., Courbaud, B., 2015. Overyielding in mixed forests decreases with site productivity. *Journal of Ecology* 103, 502–512. doi:[10.1111/1365-2745.12353](https://doi.org/10.1111/1365-2745.12353).
- Trogisch, S., Liu, X., Rutten, G., Xue, K., Bauhus, J., Brose, U., Bu, W., Cesarz, S., Chesters, D., Connolly, J., Cui, X., Eisenhauer, N., Guo, L., Haider, S., Härdtle, W., Kunz, M., Liu, L., Ma, Z., Neumann, S., Sang, W., Schuldt, A., Tang, Z., van Dam, N.M., von Oheimb, G., Wang, M.Q., Wang, S., Weinhold, A., Wirth, C., Wubet, T., Xu, X., Yang, B., Zhang, N., Zhu, C.D., Ma, K., Wang, Y., Bruelheide, H., 2021. The significance of tree-tree interactions for forest ecosystem functioning. *Basic and Applied Ecology* 55, 33–52. doi:[10.1016/j.baae.2021.02.003](https://doi.org/10.1016/j.baae.2021.02.003).
- Trumbore, S., Brando, P., Hartmann, H., 2015. Forest health and global change. *Science* 349, 814–818. doi:[10.1126/science.aac6759](https://doi.org/10.1126/science.aac6759).



- Vidal, J.P., Martin, E., Franchistéguy, L., Baillon, M., Soubeyroux, J.M., 2010. A 50-year high-resolution atmospheric reanalysis over France with the Safran system. *International Journal of Climatology* 30, 1627–1644. doi:[10.1002/joc.2003](https://doi.org/10.1002/joc.2003).
- Vilà, M., Vayreda, J., Comas, L., Ibáñez, J.J., Mata, T., Obón, B., 2007. Species richness and wood production: a positive association in Mediterranean forests. *Ecology Letters* 10, 241–250. doi:[10.1111/j.1461-0248.2007.01016.x](https://doi.org/10.1111/j.1461-0248.2007.01016.x).
- Zeller, L., Pretzsch, H., 2019. Effect of forest structure on stand productivity in Central European forests depends on developmental stage and tree species diversity. *Forest Ecology and Management* 434, 193–204. doi:[10.1016/j.foreco.2018.12.024](https://doi.org/10.1016/j.foreco.2018.12.024).
- Zhang, Y., Chen, H.Y.H., Reich, P.B., 2012. Forest productivity increases with evenness, species richness and trait variation: a global meta-analysis. *Journal of Ecology* 100, 742–749. doi:[10.1111/j.1365-2745.2011.01944.x](https://doi.org/10.1111/j.1365-2745.2011.01944.x).